PHYSICAL REVIEW B **87**, 075410 (2013)

Giant circular dichroism of a molecule in a region of strong plasmon resonances between two neighboring gold nanocrystals

Hui Zhang[*] and A. O. Govorov[†]
Department of Physics and Astronomy, Ohio University, Athens, Ohio 45701, USA

(Received 24 March 2012; published 7 February 2013)

We report on giant circular dichroism (CD) of a molecule inserted into a plasmonic hot spot. Naturally occurring molecules and biomolecules typically have CD signals in the UV range, whereas plasmonic nanocrystals exhibit strong plasmon resonances in the visible spectral interval. Therefore, excitations of chiral molecules and plasmon resonances are typically off-resonant. Nevertheless, we demonstrate theoretically that it is possible to create strongly enhanced molecular CD utilizing the plasmons. This task is doubly challenging since it requires both creation and enhancement of the molecular CD in the visible region. We demonstrate this effect within the model which incorporates a chiral molecule and a plasmonic dimer. The associated mechanism of plasmonic CD comes from the Coulomb interaction, which is greatly amplified in a plasmonic hot spot. An important feature of the system is anisotropy that results in giant enhancement for the molecular dipoles parallel to the dimer axis. The proposed effect offers very interesting possibilities for enhanced sensing of chiral molecules using visible light.

DOI: 10.1103/PhysRevB.87.075410 PACS number(s): 78.67.Bf, 71.35.Cc, 73.20.Mf

I. INTRODUCTION

Plasmon resonances in metal nanostructures provide us with powerful methods of molecular spectroscopy. One impressive example is surface enhanced Raman scattering (SERS), allowing the observation of vibrational spectra of single molecules.[1,2] The physical mechanism of enhancement in SERS comes from amplification of electromagnetic fields in so-called plasmonic hot spots of metal nanocrystals. Another related example is an effect of plasmon-enhanced emission of dye molecules in the vicinity of metal nanoparticles (NPs).[3] Circular dichroism (CD) is an optical technique very different from the methods mentioned above. A CD spectrum is measured as a difference in absorbance of right-handed and left-handed circularly-polarized photons. Importantly, CD is sensitive to the symmetry of a molecule;[4] more precisely, a CD spectrum tells us about the chiral property of a molecular object. Historically the CD method has been very successful in applications to biomolecules and drugs.[4] For example, it was a powerful method to differentiate a secondary structure of proteins which can appear in the forms of α helix, random coil, or β sheet. Recently the concepts of chirality and CD have been brought to the field of plasmonics.[5–22] One of the motivations for this development is plasmon-enhanced sensing of chiral molecules.

Here we show theoretically that the chiral property of a molecule can be both strongly enhanced and transferred to the visible wavelength range by using a plasmonic hot spot in a nanoparticle dimer [Fig. 1(a)]. For oriented molecules, the calculated enhancement factors of CD are 12 and 150 for the Au and Ag systems, respectively. For randomly oriented chiral molecules, the enhancements are smaller, 4- and 12-fold. It is important that the enhancement effect is accomplished by the transfer of the CD signal from the UV to the visible-wavelength plasmonic resonances. Our results are in agreement with a recent experiment on nanocrystal aggregates and short DNA molecules.[11] In particular, this experimental paper[11] identified the aggregation of nanocrystals as a condition to observe enhanced plasmonic CD. Aggregates are expected to have hot plasmonic spots in gaps between nanocrystals. We also should note that our previous calculations have been performed mostly for single nanocrystals or dimers with relatively large separations in the dipole regime of interaction.[12,23] Such systems did not have plasmonic hot spots with giant enhancement and, as a result, we did not predict plasmon enhancement of CD, but we found an important effect of transfer of molecular chirality to the plasmon resonances; the plasmonic CD effect has been recently observed in experiments with Au NPs and chiral molecules.[14] As an important next step in future developments, the plasmon enhancement effect can be extended to the concept of Raman optical activity.[24]

II. MODEL

A molecule–gold-dimer hybrid system [Fig. 1(a)] is excited by an incident light wave with an electric field $\mathbf{E}_{\text{ext}} = \mathbf{E}_0 e^{-i\omega t} + \mathbf{E}_0^* e^{i\omega t}$, where $\mathbf{E}_0$ is an amplitude; correspondingly, the magnetic field amplitude $\mathbf{B}_0 = \frac{\sqrt{\epsilon_{r,0}}}{c}\mathbf{k}_0 \times \mathbf{E}_0/k_0$. Here $\epsilon_{r,0}$ and $k_0 = 2\pi/\lambda$ are the relative dielectric constant of matrix (water) and the photon wave number in vacuum, respectively. We consider here the quasielectrostatic case, i.e., $\lambda \gg D$, where D is a size of the system. Then, the master equation for the quantum states of molecule reads

$$\hbar\frac{\partial \rho_{ij}}{\partial t} = i[\hat{\rho},\hat{H}]_{ij} - \Gamma_{ij}(\rho), \tag{1}$$

where $\hat{H} = \hat{H}_0 + \hat{H}'$ is the Hamiltonian and $\hat{\rho}$ is the density matrix. Here H_0 describes the internal electronic structure of a molecule and $\hat{H}' = -\hat{\boldsymbol{\mu}} \cdot \mathbf{E}_T - \hat{\mathbf{m}} \cdot \mathbf{B}_T + V_{\text{quad}}$ is the light-matter interaction operator;[24] $\mathbf{E}_T$ and $\mathbf{B}_T$ are the fields acting on the molecule, and $\hat{\boldsymbol{\mu}}$ and $\hat{\mathbf{m}}$ stand for the electric and magnetic dipolar operators, respectively: $\hat{\boldsymbol{\mu}} = e\hat{\mathbf{r}}$, $\hat{\mathbf{m}} = \frac{e}{2m_e}\hat{\mathbf{r}} \times \hat{\mathbf{p}}$; V_{quad} is the quadrupole interaction defined in the Supplemental Materials.[25] By using the rotating-wave approximation in the linear regime and involving only two states (1 and 2), we obtain from Eq. (1) (see

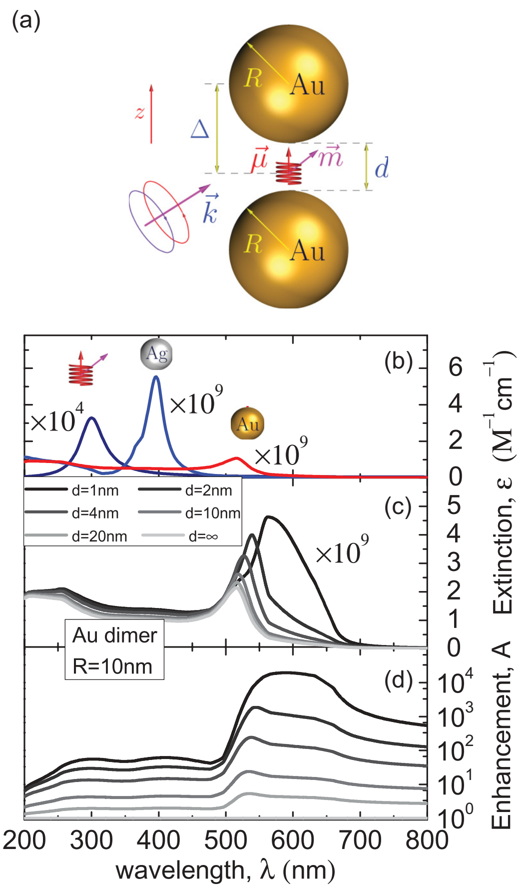

FIG. 1. (Color online) (a) Schematics of a model incorporating a gold dimer and a chiral molecule. (b) Extinctions of single-molecule and single noble metal NPs. (c) Extinction of an Au dimer for various separations d. (d) Enhancement factor A vs the wavelength of incident light in the center of a gold dimer in the absence of molecule. The parameters are $\mathbf{E}_0||z$, molecular resonance $\lambda_0 = 300$ nm.

Appendix A)

$$
\begin{aligned}
\rho_{21} &= \sigma_{21} e^{-i\omega t}, \quad \rho_{12} = \rho_{21}^{*}, \quad \mathbf{d} = \sigma_{21}\boldsymbol{\mu}_{12},\\
\sigma_{21} &= -\frac{\boldsymbol{\mu}_{21}\cdot\mathbf{E}' + \mathbf{m}_{21}\cdot\mathbf{B}'}{\hbar(\omega-\omega_0) + i\gamma_{21} - G},\\
\rho_{22} &= \frac{2\gamma_{21}}{\gamma_{22}} \frac{|\boldsymbol{\mu}_{21}\cdot\mathbf{E}' + \mathbf{m}_{21}\cdot\mathbf{B}'|^2}{|\hbar(\omega-\omega_0) + i\gamma_{21} - G|^2},
\end{aligned}
\tag{2}
$$

where $\hbar\omega_{1(2)}$ are the energies of the molecular states, $\omega_0 = \omega_2 - \omega_1$ is the frequency of molecular transition, and $\mathbf{E}'$ is the electric field induced by the incident wave in the nanostructure at the position of a molecule. This electric field includes the external field and the plasmonic field induced by NPs. The magnetic field in a small structure is not affected much by the plasmonic effects, i.e., $\mathbf{B}' \approx \mathbf{B}_0$.[12] In addition, the broadening function $G = \frac{1}{4\pi\epsilon_0}\boldsymbol{\mu}_{21}\cdot\nabla(\boldsymbol{\Phi}_\omega\cdot\boldsymbol{\mu}_{12}) + G_{\text{quad}}$, where the vector $\boldsymbol{\Phi}_\omega$ defines the electric potential Φ_d which is induced by the surface charges of NPs in the presence of an oscillating molecular dipole $\mathbf{d}$; then, the function $\varphi_d = \frac{1}{4\pi\epsilon_0}(\frac{\mathbf{d}\cdot\mathbf{r}}{r^3} + \Phi_d)$ gives the total electric potential induced by the molecular dipole in the presence of NPs, and $\Phi_d = \mathbf{d}\cdot\boldsymbol{\Phi}_\omega$. Thus, the total field acting on a molecule is given by $\mathbf{E}_T = \mathbf{E}' - \frac{1}{4\pi\epsilon_0}\nabla\Phi_d$. The function G in Eqs. (2) originated from the plasmonic surface charges induced by the molecular dipole $\mathbf{d}$. Then, the total absorption rate of the system is

$$
Q = Q_{\text{mol}} + Q_{\text{NP}}, \tag{3}
$$

where $Q_{\text{NP}} = 2\omega\text{Im}\epsilon_{\text{NP}}\int_{\text{NPs}}|\mathbf{E}_{\text{tot}}|^2 dV$ and $Q_{\text{mol}} = \omega_0\rho_{22}\gamma_{22}$, in which ϵ_{NP} is the permittivity of NPs ($\epsilon_{NP} = \epsilon_{r,NP}\epsilon_{\text{vac}}$), the integral is taken over NP volumes, and $\mathbf{E}_{\text{tot}}$ denotes the total field inside NPs. A CD signal is defined as the difference between absorption of left- and right-handed polarized light,

$$
\text{CD} = \langle Q_+ - Q_- \rangle_\Omega = \text{CD}_{\text{mol}} + \text{CD}_{\text{NP}}, \tag{4}
$$

where $\langle\cdots\rangle_\Omega$ is the average over the solid angle of the direction of incident light; this averaging is equivalent to what happens in experiments performed in solution: hybrid NP complexes have random orientations, but the incident light has a well defined direction. Also, ± denotes the two polarizations of incident field $\mathbf{e}_{0\pm} = (\mathbf{e}_\theta \pm i\mathbf{e}_\phi)/\sqrt{2}$. Since the total field inside NPs is $\mathbf{E}_T = \mathbf{E}' - \nabla\varphi_d$, the important plasmonic contribution Q_{NP} can be split into four terms, $Q_{\text{NP}} = Q_0 + Q_{\text{NP, diople-field}} + Q_{\text{NP, dipole-dipole}} + Q_{\text{NP, quad}}$, where Q_0 is the absorption by the NP dimer,

$$
\begin{aligned}
Q_{\text{NP, dipole-field}} &= -\frac{\omega}{\pi\epsilon_0}\text{Im}[\epsilon_{\text{NP}}]\text{Re}\int_{\text{NPs}} dV(\mathbf{E}'^{*}\cdot\nabla\varphi_d),\\
Q_{\text{NP, dipole-dipole}} &= \frac{\omega}{8\pi^2\epsilon_0^2}\text{Im}[\epsilon_{\text{NP}}]\int_{\text{NPs}} dV\,|\nabla\varphi_d|^2\,,
\end{aligned}
\tag{5}
$$

Therefore, the CD_{NP} should have three terms since the NP system itself is nonchiral and Q_0 does not give contribution to CD. Finally, we arrive at (see Appendix C)

$$
\begin{aligned}
\text{CD}_{\text{mol}} &= \frac{8\sqrt{\epsilon_r}}{3c}\frac{\omega_0\gamma_{21}|E_0|^2\text{Im}[\mathbf{m}_{21}\cdot(\hat{\mathcal{P}}^{\dagger}\boldsymbol{\mu}_{12})]}{|\hbar(\omega-\omega_0) + i\gamma_{21} - G|^2}\\
&\quad + \text{CD}_{\text{mol, quad}},\\
\text{CD}_{\text{NP}} &= \text{CD}_{\text{NP, dipole-field}} + \text{CD}_{\text{NP, dipole-dipole}}\\
&\quad + \text{CD}_{\text{NP, quad-field}},\\
\text{CD}_{\text{NP, dipole-field}} &= \frac{2\omega\sqrt{\epsilon_r}}{3c\pi\epsilon_0}|E_0|^2(\text{Im}\epsilon_{\text{NP}})\\
&\quad \times\text{Im}\int_{\text{NPs}}\frac{\mathbf{m}_{21}\cdot[\hat{K}^{\dagger}(\mathbf{r})\nabla(\boldsymbol{\Phi}^{\text{tot}}(\mathbf{r})\cdot\boldsymbol{\mu}_{21})]}{\hbar(\omega-\omega_0) + i\gamma_{21} - G}dV,\\
\text{CD}_{\text{NP, dipole-dipole}} &= -\frac{8\omega\sqrt{\epsilon_r}}{3c}\frac{|E_0|^2\text{Im}[\mathbf{m}_{21}\cdot(\hat{\mathcal{P}}^{\dagger}\boldsymbol{\mu}_{12})]}{|\hbar(\omega-\omega_0) + i\gamma_{21} - G|^2}\text{Im}G,
\end{aligned}
\tag{6}
$$

where $\hat{\mathcal{P}}$ and $\hat{K}(\mathbf{r})$ are the field-enhancement matrices inside a molecule and NPs, respectively (see Appendix B): $\mathbf{E}'|_{\mathbf{r}=\mathbf{r}_{\text{mol}}} = \hat{\mathcal{P}}\mathbf{E}_0$, $\mathbf{E}'(\mathbf{r}) = \hat{K}(\mathbf{r})\mathbf{E}_0$ ($\mathbf{r} \in$ NPs). Also, $\boldsymbol{\Phi}^{\text{tot}}$ is the total electric potential induced by dipole $\mathbf{d}$ inside NPs: $\boldsymbol{\Phi}^{\text{tot}} = \frac{\mathbf{r}}{r^3} + \boldsymbol{\Phi}_\omega$.

In our study, we solve numerically the near-field Poisson equation within the local dielectric constant model and beyond the dipole limit. We expand the electric potentials coming from the induced surface charges of NPs and the external field in terms of spherical harmonics.[26] For example, the potential induced by surface charges of one of the NPs can be written as $\boldsymbol{\Phi}_\omega^{\text{out}} = \sum_{l,m}\frac{\mathbf{C}_{lm}}{r^{l+1}}Y_l^m(\theta,\phi)$, where $\mathbf{C}_{lm} = (C_{lm}^x, C_{lm}^y, C_{lm}^z)$ are coefficients found from the boundary conditions. This method allows us to compute metal nanostructures with very strong plasmonic enhancements (Fig. 1). The convergence of the multipole expiation method was carefully checked; the number $L_{\max}$ in the calculations was around 50 for $d = 1$ nm and 120 for $d = 0.5$ nm.

For the molecular dipole, we choose numbers typical for the experiments. We first define convenient parameters: $\mu_{12} = |e|r_{12}$ and $\boldsymbol{\mu}_{12} \cdot \mathbf{m}_{21}/\mu_{12} = i|e|r_0\omega_0 r_{21}/2$. In our calculations, we use $r_{12} = 2$ Å, $r_0 = 0.05$ Å, $\gamma_{12} = 0.3$ eV. The key chiral parameter r_0 determines a CD strength of a molecule:[4] $\mathrm{CD}_{\mathrm{mol},0} \sim \mathrm{Im}(\boldsymbol{\mu}_{12} \cdot \mathbf{m}) \sim r_0$. The parameter r_0 is a small number since chirality of a molecule is usually weak. The above parameters of a chiral molecule yield typical numbers for the molecular extinction and CD. For the dielectric functions of metals (Au and Ag), Palik's data[27] were adopted; the optical dielectric constant of the matrix (water) $\epsilon_{r,0} = 1.8$.

III. NUMERICAL RESULTS AND DISCUSSIONS

First, we briefly discuss optical properties of the constituting elements [Fig. 1 (b)]. Molecules and biomolecules usually have CD lines in the UV or near-UV range. In Fig. 1(b) we show an example of extinction spectrum of a molecule with a resonance at 300 nm. Its maximum is $\sim 10^4$ $\mathrm{M}^{-1}\mathrm{cm}^{-1}$, which is a typical value for molecular systems. Extinctions of noble metal NPs (Au and Ag) are much larger and have plasmon resonances in the visible range (520 and 400 nm). Moreover, plasmonic NP complexes demonstrate both red shifts of plasmon peaks and remarkable enhancement of incident electromagnetic fields [Figs. 1(c) and 1(d)]. Especially strong enhancement occurs in the plasmonic hot spots,[28–30] i.e., in the center of the dimer. The calculated enhancement factor $A = |\mathbf{E}'|^2/|\mathbf{E}_0|^2$ can be as large as 10^4 for small separations d.

Now we turn to the CD effect and first consider an off-resonant hybrid system with a gold dimer and a molecular resonance at $\lambda_0 = 300$ nm (Fig. 2). If a chiral molecule is placed in the vicinity of a single metal NP, the resultant CD spectrum acquires plasmon structures, but the strength of these structures is typically moderate[12,14] [Fig. 2(a)]. A sign of the plasmonic CD depends on the orientation of molecular dipole. Remarkably different spectra appear for the chiral molecule in a metal NP dimer with small separations d (Figs. 2 and 3). For the Au dimer with ($\boldsymbol{\mu}_{12}||z$), [Fig. 2(b)], we obtain the following picture: The molecular CD band at 300 nm is now transformed into an asymmetric structure and the plasmonic CD structure becomes very strong and broad. The first effect (i.e., the UV-CD structure) comes from the interference of incident and induced fields (Fano effect),[30–32] whereas the second originates from the giant enhancement of electric field at the chiral molecule and from Coulomb interaction between a chiral object (molecule) and a nonchiral plasmonic nanostructure. We now introduce a figure of merit for the plasmon enhancement of CD:

$$P_{\mathrm{CD}} = \frac{\mathrm{CD}_{\max}(\lambda = \lambda_{\mathrm{plasm}})}{\mathrm{CD}_{\mathrm{mol},0,\max}(\lambda = \lambda_0)}. \tag{7}$$

This enhancement factor, which compares a CD signal in the plasmonic band with the original molecular CD at 300 nm, is ~ 12. We also note that the plasmonic CD structure is broad because the interparticle Coulomb interaction allows for excitation of many multipole modes of single NPs. For the other orientation ($\boldsymbol{\mu}_{12} \perp z$), the plasmonic CD band is weak because of the screening effect. The CD spectrum averaged over the orientation of the molecule should be calculated as $\langle \mathrm{CD} \rangle = (\mathrm{CD}_z + \mathrm{CD}_x + \mathrm{CD}_y)/3 \approx \mathrm{CD}_z/3$. This spectrum still has a strong plasmon resonance (enhancement factor ~ 4). Remarkably, this enhancement is comparable with the experimental data[11] obtained for aggregated Au NPs and short DNA molecules [inset of Fig. 2(d)]. Figure 2(c) also shows the contribution of the quadrupole interaction. Overall we found that the quadrupole effect in a molecule is not enhanced by a plasmonic dimer and, due to the symmetry of the dimer, can play a role only for the configurations $\boldsymbol{\mu}||x(y)$ (For details, see the Supplemental Materials[25]). We note that the quadrupole CD signal from randomly oriented molecules in a solution is averaged to zero.[24,33] In our case, the quadrupole effect in the CD spectrum remains nonzero because of the anisotropy of a plasmonic dimer.

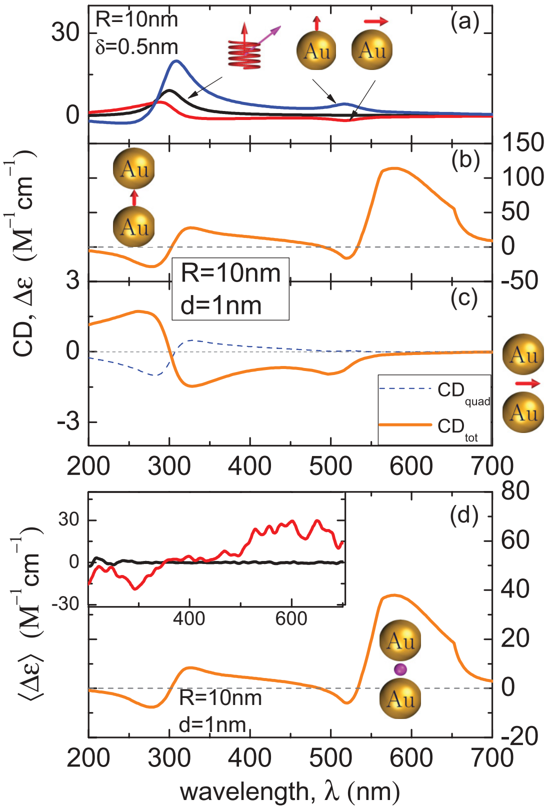

FIG. 2. (Color online) (a) CD spectra for an isolated molecule and for molecule–single-NP complexes with two orientations of a molecular dipole: $\boldsymbol{\mu}||z$ and $\boldsymbol{\mu}||x$. (b), (c) CD signals for the molecule–Au-dimer complexes with different molecular orientations. (d) CD signal for the molecule–Au-dimer complex averaged over the molecular dipole orientation; the inset shows experimental data obtained in Ref. 11. The parameters of the calculation are $R = 10$ nm, $d = 1$ nm, $\lambda_0 = 300$ nm, $\Delta = R + d/2$.

Figure 3 shows CD spectra for the Ag nanostructure which has much stronger plasmonic enhancement since the Ag plasmon resonance is much sharper. In this case, the configuration with $\boldsymbol{\mu}||z$ has a CD enhancement factor of 150 for $d = 0.5$ nm and an averaged CD is enhanced 12-fold for $d = 1$ nm.

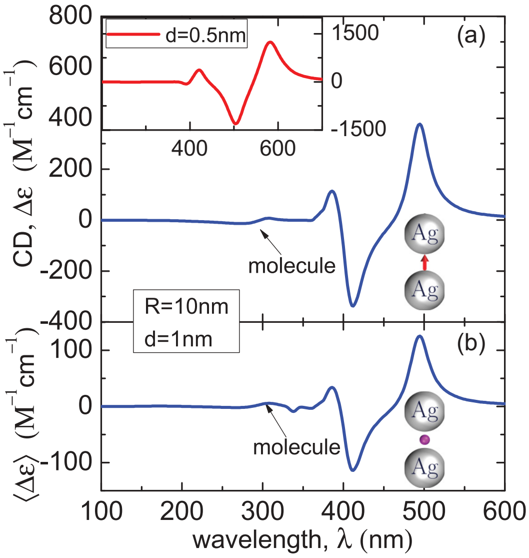

FIG. 3. (Color online) (a) CD spectrum of an Ag dimer for $d = 1$ nm in the case $\boldsymbol{\mu}||z$. The inset shows the CD signal for the separation $d = 0.5$ nm. (b) CD spectrum of an Ag dimer averaged over the molecular orientation. The parameters are $R = 10$ nm and $\lambda_0 = 300$ nm.

Some of the biomolecules may have CD signals also in the blue spectral interval.[34] This case is shown now in Fig. 4. A molecule with $\lambda_0 = 400$ nm is located in the center of an Ag dimer. The following effects should be now noticed: (a) the CD spectrum is amplified 125-fold; (b) multipole plasmon resonances in the Ag dimer create a broad CD spectrum with positive and negative bands; and (c) a strong plasmonic CD signal appears at 500 nm which is a significantly longer wavelength compared with the original molecular CD wavelength of 400 nm. In other words, we again observe simultaneously a strong enhancement effect and a creation of the optical chirality in the red. Regarding the feature (b), we confirm the explanation for this effect by looking at the absorption spectrum of Ag dimer which indeed has strong multipole resonances in the interval 400–500 nm. Similar results can be obtained for the Au dimer.

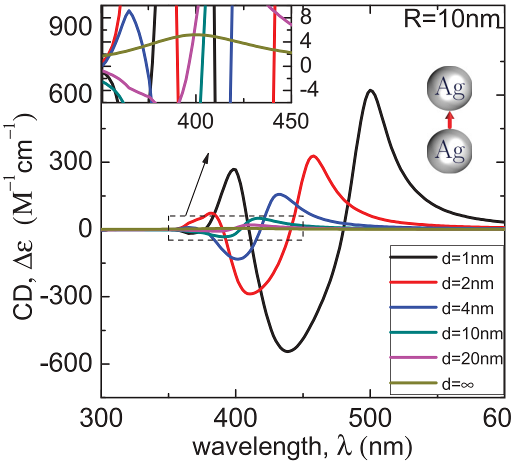

FIG. 4. (Color online) CD spectrum of an Ag dimer for the molecular resonance $\lambda_0 = 400$ nm and for various separations d. Inset: Small region of the spectrum.

We now look at the mechanism of the enhanced plasmonic CD. Numerical data (see Appendix D) indicate that for the most common case (off-resonant exciton-plasmon regime), as shown in Figs. 2 and 3, the leading term in the CD signal is $\mathrm{CD}_{\text{dipole-field}}$. This is the term coming from the interference of the incident field and the field induced by a chiral molecular dipole inside the NPs. In the off-resonant regime ($\omega_0 - \omega_{\text{plasm}} \gg \gamma_{12}, |G|$), a CD signal in the plasmonic band is proportional the optical rotatory dispersion (ORD) of a molecule

$$\mathrm{CD}_{\text{dipole-field}} \sim f(\omega) \times \mathrm{ORD}_{\text{mol},0} \sim f(\omega)\frac{m_{12}\mu_{21}}{\omega_0 - \omega_{\text{plasm}}}, \quad (8)$$

where $f(\omega)$ is a complex function describing the energy dissipation inside the metal in the vicinity of molecule placed in a plasmonic hot spot. Since the function $f(\omega)$ comes from the induced dissipative currents inside the plasmonic NPs, we expect that this function should be greatly amplified at the plasmon resonances because of the enhancement of the electric fields in a hot spot. Indeed we see this effect in our data (Figs. 2 and 3). In our physical model, the enhanced CD originates from a joint action of the two key effects: the ORD response of a chiral molecule at the plasmon wavelength and the plasmonic hot spot effect. We should note here that the molecule itself does not absorb at the plasmon resonance. Therefore, the giant CD at the plasmon wavelength comes from the dissipation inside the metal subsystem. The plasmon resonances of nonchiral metal NPs interact with a chiral nonabsorbing environment (a chiral molecule in the hot spot) and therefore acquire a chiral property, and demonstrate CD. In our theory, this effect originates from the term $\mathrm{CD}_{\text{NP,dipole-field}}$ in the general equation for CD. This term describes the energy dissipation inside metal NPs due to the joint action of the dipolar field of a chiral molecule and the external field. Since both dipolar and external fields are greatly enhanced in the vicinity of a hot spot, this term in CD shows very strong enhancement. The functions $G(\omega)$ and $\mathrm{CD}_{\text{NP,dipole-dipole}}$ play an essential role only for small d when the molecule-surface distance is small. $G(\omega)$ generates broadening of the molecular resonance and $\mathrm{CD}_{\text{NP,dipole-dipole}}$ appears due to the dissipation inside the metal induced by the molecular dipolar field. Another qualitative observation is that the plasmonic CD decreases with $\omega_0 - \omega_{\text{plasm}}$ since it depends on the molecular ORD at the plasmonic frequency [Eq. (8)]. Notably, for separation $d = 1$ nm the influence of quantum effects is very small,[35] so that our plasmonic subsystem can be described by the classical theory of the local dielectric function and is within the classical regime.

IV. CONCLUSION

To conclude, we have presented a theory of optical activity of a chiral molecule inserted into a plasmonic hot spot and we have found an important effect: simultaneous strong plasmonic enhancement and shift of optical chirality from the UV range to the visible. The mechanism of enhanced plasmonic CD signals is based on the Coulomb interaction between a chiral molecules and plasmonic modes in a hot spot. The

Coulomb interaction inside the molecule-NP complex is highly anisotropic that creates strong plasmonic enhancement only for the molecular dipoles parallel to the dimer axis. Therefore, an orientation of molecular dipoles in a dimer should be along the dimer axis to obtain strong CD in the visible. This property can be crucial for designing anisotropic molecular-plasmonic structures with strong induced CD at the plasmon wavelength. Importantly, single spherical NPs are not able to create any significant enhancement of CD signals and, therefore, the use of plasmonic hot spots is crucial for the ultrasensitive CD spectroscopy. The effect of strong plasmonic CD in the visible range, which is described here, can be utilized for chiral biosensing and also for construction of novel chiral optically active materials.

ACKNOWLEDGMENTS

This work was supported by the Volkswagen Foundation and the NSF (Project no. CBET-0933415).

APPENDIX A: ABSORPTION RATE OF CHIRAL MOLECULE

Next we shall derive the formula Eq. (2) in the paper. The master equation for the quantum states of molecule is given by

$$\hbar\frac{\partial\rho_{ij}}{\partial t} = i[\rho,\hat{H}] - \Gamma_{ij}(\rho) \tag{A1}$$

in which $\hat{H} = \hat{H}_0 + \hat{H}'$ is the Hamiltonian, and $\hat{H}' = (-\hat{\boldsymbol{\mu}}\cdot\mathbf{E}_T - \hat{\mathbf{m}}\cdot\mathbf{B}_T)$ where the total field are respectively $\mathbf{E}_T = \mathbf{E}_{\text{tot}}e^{-i\omega t} + \mathbf{E}^*_{\text{tot}}e^{i\omega t}$ and $\mathbf{B}_T = \mathbf{B}_{\text{tot}}e^{-i\omega t} + \mathbf{B}^*_{\text{tot}}e^{i\omega t}$. Here, $\mathbf{E}_T,\mathbf{B}_T$ are the total electromagnetic fields inside the chiral molecule. Also, $\boldsymbol{\mu} = e\mathbf{r}$, $\mathbf{m} = \frac{e}{2m_e}\mathbf{r}\times\mathbf{p}$ stand for the electric and magnetic dipolar operators, respectively. $\Gamma_{ij}(\rho)$ is the relaxation term, and if we only involve two quantum states, it will be given by $\Gamma_{11}(\rho) = -\Gamma_{22}(\rho) = -\gamma_{22}\rho_{22},\Gamma_{12}(\rho) = \gamma_{21}\rho_{12},\Gamma_{21}(\rho) = \gamma_{21}\rho_{21}$. Here we note that the effects of the quadrupole light-matter interaction will be discussed separately in the Supplemental Materials.[25] Then, after substituting H into (A1), one has

$$\hbar\frac{\partial\rho_{21}}{\partial t} = -i\hbar\omega_0\rho_{21} + i(\rho_{11}-\rho_{22})(\boldsymbol{\mu}_{21}\cdot\mathbf{E}_T + \mathbf{m}_{21}\cdot\mathbf{B}_T) - \gamma_{21}\rho_{21}, \tag{A2}$$

$$\hbar\frac{\partial\rho_{22}}{\partial t} = -i(\rho_{21}\boldsymbol{\mu}_{12} - \boldsymbol{\mu}_{21}\rho_{12})\cdot\mathbf{E}_T - i(\rho_{21}\mathbf{m}_{12} - \mathbf{m}_{21}\rho_{12})\cdot\mathbf{B}_T - \gamma_{22}\rho_{22}, \tag{A3}$$

where $\boldsymbol{\mu}_{i,j} = \langle i|\hat{\boldsymbol{\mu}}|j\rangle, i = 1,2$, and $\omega_0 = \omega_2 - \omega_1$. Next, we adopt the rotating-wave approximation $\rho_{21} = \sigma_{21}e^{-i\omega t},\rho_{12} = \rho^*_{21}$ and only keep the $e^{-i\omega t}$ time dependence in Eqs. (A2) and (A3), thus Eqs. (A2) and (A3) become

$$\hbar\frac{\partial\sigma_{21}}{\partial t} \approx [i\hbar(\omega-\omega_0) - \gamma_{21}]\sigma_{21} + i(\rho_{11}-\rho_{22})(\boldsymbol{\mu}_{21}\cdot\mathbf{E}_{\text{tot}} + \mathbf{m}_{21}\cdot\mathbf{B}_{\text{tot}}), \tag{A4}$$

$$\hbar\frac{\partial\rho_{22}}{\partial t} \approx -i[\sigma_{21}(\boldsymbol{\mu}_{12}\cdot\mathbf{E}^*_{\text{tot}} + \mathbf{m}_{12}\cdot\mathbf{B}^*_{\text{tot}}) - \sigma_{12}(\boldsymbol{\mu}_{21}\cdot\mathbf{E}_{\text{tot}} + \mathbf{m}_{21}\cdot\mathbf{B}_{\text{tot}})] - \gamma_{22}\rho_{22}. \tag{A5}$$

Since σ_{21} is a new "slowly" varying variable, thus we have $\hbar\frac{\partial\sigma_{21}}{\partial t} \approx 0$ and $\hbar\frac{\partial\rho_{22}}{\partial t} \approx 0$. Furthermore, $\mathbf{E}_{\text{tot}}$ inside the molecule can be divided into two parts: $\mathbf{E}_{\text{tot}} = \mathbf{E}' + \mathbf{E}_d,\mathbf{E}' \equiv \mathbf{E}_0 + \mathbf{E}_{\text{ind}}$, where $\mathbf{E}_0$ is the incident field, $\mathbf{E}_{\text{ind}}$ is the electric field induced by NPs in the absence of a chiral molecule, and $\mathbf{E}_d$ is the electric field coming from charges in the surfaces of NPs induced only by the molecule. Notably, in the presence of electromagnetic filed, a molecular dipole moment $\mathbf{d}_{\text{mol}} = \text{Tr}(\rho\boldsymbol{\mu}) = \mathbf{d}e^{-i\omega t} + \mathbf{d}^*e^{i\omega t}$ will be induced where $\mathbf{d} = \sigma_{21}\boldsymbol{\mu}_{12}$, and accordingly $\mathbf{E}_d$ has the following form:

$$\mathbf{E}_d = -\frac{1}{4\pi\epsilon_0}\nabla(\boldsymbol{\Phi}_\omega\cdot\mathbf{d}) = -\frac{1}{4\pi\epsilon_0}\nabla(\boldsymbol{\Phi}_\omega\cdot\boldsymbol{\mu}_{12})\sigma_{21}, \tag{A6}$$

where ϵ_0 is the electric permittivity of space, and we adopt the Palik data hereafter. Therefore, Eq. (A4) gives us

$$\begin{aligned} 0 &\approx [i\hbar(\omega-\omega_0) - \gamma_{21}]\sigma_{21} + i(\rho_{11}-\rho_{22}) \\ &\quad\times\left[\boldsymbol{\mu}_{21}\cdot\left(\mathbf{E}' - \frac{1}{4\pi\epsilon_0}\nabla(\boldsymbol{\Phi}_\omega\cdot\boldsymbol{\mu}_{12})\sigma_{21}\right) + \mathbf{m}_{21}\cdot\mathbf{B}'\right] \\ &\Rightarrow \sigma_{21} = -\frac{(\rho_{11}-\rho_{22})(\boldsymbol{\mu}_{21}\cdot\mathbf{E}' + \mathbf{m}_{21}\cdot\mathbf{B}')}{\hbar(\omega-\omega_0) + i\gamma_{21} - (\rho_{11}-\rho_{22})G} \end{aligned} \tag{A7}$$

where the G function is defined as $G = \frac{1}{4\pi\epsilon_0}\boldsymbol{\mu}_{21}\cdot\nabla(\boldsymbol{\Phi}_\omega\cdot\boldsymbol{\mu}_{12})$ and we have used $\mathbf{B}_{\text{tot}} \approx \mathbf{B}' \approx \mathbf{B}_0$. Similarly, from (A5) we have

$$\rho_{22} = \frac{2\gamma_{21}}{\gamma_{22}}\frac{(\rho_{11}-\rho_{22})|\boldsymbol{\mu}_{21}\cdot\mathbf{E}' + \mathbf{m}_{21}\cdot\mathbf{B}'|^2}{|\hbar(\omega-\omega_0) + i\gamma_{21} - (\rho_{11}-\rho_{22})G|^2}. \tag{A8}$$

In the linear regime $\rho_{22} \ll 1$, Eqs. (A7) and (A8) reduce to the formula Eq. (2) in the paper. Finally, by using $Q_{\text{mol}} = \omega_0\rho_{22}\gamma_{22}$, the absorption rate of the chiral molecule in the linear regime is given by

$$Q_{\text{mol}} = 2\omega_0\gamma_{21}\frac{|\boldsymbol{\mu}_{21}\cdot\mathbf{E}' + \mathbf{m}_{21}\cdot\mathbf{B}'|^2}{|\hbar(\omega-\omega_0) + i\gamma_{21} - G|^2}. \tag{A9}$$

APPENDIX B: GENERAL DIELECTRIC FORMALISM

The general dielectric formalism of a molecule–NP-dimer complex reads as follows:

$$\nabla\cdot\epsilon\nabla\phi_{\text{ind}} = \nabla\cdot\epsilon\mathbf{E}_0, \quad \nabla\cdot\epsilon\nabla\varphi_d = \rho_d, \tag{B1}$$

where ϵ denotes the dielectric function of the medium and NPs, ϕ_{ind} is the electric potential induced by NPs in the absence of a molecule, $\mathbf{E}_0$ is the incident field, φ_d is the electric potential of the complex only induced by molecular dipole $\mathbf{d}$ in the absence of an incident field, while ρ_d is the charge inside molecule. Then, in the absence of a molecule, the total electric field is given by $\mathbf{E}' = -\nabla\phi_{\text{ind}} + \mathbf{E}_0$, and the enhancement matrices can be defined as

$$\mathbf{E}'|_{\mathbf{r}=\mathbf{r}_{\text{mol}}} = \hat{\mathcal{P}}\mathbf{E}_0; \quad \mathbf{E}'(\mathbf{r}) = \hat{\mathcal{K}}\mathbf{E}_0 \quad (\mathbf{r}\in\text{NPs}). \tag{B2}$$

$\hat{\mathcal{P}}$ and $\hat{\mathcal{K}}$ are very useful for the following derivations. Similarly, from the second equation of (B1), we can obtain the G function as well as the electric potential induced by the molecular dipole φ_d. In Fig. 5 we show the enhancement factor $A = |\mathcal{P}|^2$ in the hot spot of Au and Ag dimers.

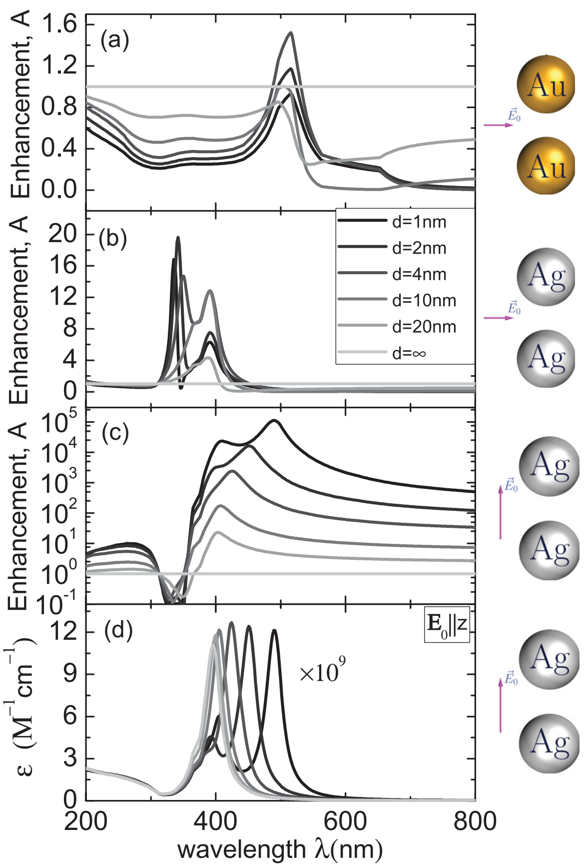

FIG. 5. (Color online) (a) Enhancement factor A vs the wavelength of incident light in the hot spot of an Au dimer under the incident light $\mathbf{E}_0||x$. (b), (c) Respectively, the enhancement factor A for the Ag dimer in the hot spot in the cases $\mathbf{E}_0||x$ and $\mathbf{E}_0||z$. (d) Extinction of the Ag dimer for various separations d under $\mathbf{E}_0||z$. Other unmentioned parameters are the same as Fig. 1 in the main text.

APPENDIX C: CD SIGNAL OF MOLECULE–NP-DIMER COMPLEX

Next, we shall derive the formula Eq. (6) in the paper. The CD signal refers the the difference between absorption of left- and right-handed polarized light, so that it is given by:

$$\mathrm{CD} = \langle Q_+ - Q_- \rangle_\Omega = \mathrm{CD}_{\mathrm{mol}} + \mathrm{CD}_{\mathrm{NP}}, \tag{C1}$$

where $\langle \cdots \rangle_\Omega$ is the average over the solid angle of the incident field, which is equivalent to what happens in experiments: the hybrid complex has random orientations but the incident light has well defined direction. Also, ± denotes the two polarizations of incident field $\mathbf{e}_{0\pm} = (\mathbf{e}_\theta \pm i\mathbf{e}_\phi)/\sqrt{2}$. In the following we shall calculate the two parts, i.e., $\mathrm{CD}_{\mathrm{mol}}$ and $\mathrm{CD}_{\mathrm{NP}}$.

1. CD signal of molecular part

Substituting the two polarizations into Eq. (A9), we have

$$Q_{\mathrm{mol}\pm} = \omega_0\gamma_{21}\frac{|E_0|^2|\boldsymbol{\mu}_{21}\cdot\hat{\mathcal{P}}(\mathbf{e}_\theta \pm i\mathbf{e}_\phi) + \mathbf{m}_{21}\cdot\sqrt{\epsilon_r}(\mathbf{e}_\phi \mp i\mathbf{e}_\theta)/c|^2}{|\hbar(\omega-\omega_0) + i\gamma_{21} - G|^2}$$

$$\Rightarrow \mathrm{CD}_{\mathrm{mol}} = \langle Q_{\mathrm{mol}+} - Q_{\mathrm{mol}-}\rangle_\Omega = \frac{8\sqrt{\epsilon_r}}{3c}\frac{\omega_0\gamma_{21}|E_0|^2\mathrm{Im}[\mathbf{m}_{21}\cdot(\hat{\mathcal{P}}^\dagger\boldsymbol{\mu}_{12})]}{|\hbar(\omega-\omega_0) + i\gamma_{21} - G|^2}, \tag{C2}$$

where the enhancement matrix $\hat{\mathcal{P}}$ is defined in Eq. (B2) and used the formula $\mathbf{B}' \approx \mathbf{B}_0$, $\langle|\boldsymbol{\mu}\cdot(\mathbf{e}_\theta \pm i\mathbf{e}_\phi) + \mathbf{m}\cdot(\mathbf{e}_\phi \mp i\mathbf{e}_\theta)|^2\rangle_\Omega = \frac{2}{3}|\boldsymbol{\mu} \mp i\mathbf{m}|^2$. Notably, $\mathbf{E}'$ is the actual electric field in the center of NP dimer in the absence of molecule.

Once the CD signal Eq. (C2) is obtained, we can calculate it in the standard units of $\mathrm{M}^{-1}\mathrm{cm}^{-1}$ as follows. Since the light intensity in this case is $\langle S\rangle_t = 2\epsilon_{\mathrm{vac}}c\sqrt{\epsilon_r}|\mathbf{E}_0|^2$, thus the cross section is (in units of m^2)

$$\Delta\sigma_{\mathrm{mol}} \equiv \frac{\mathrm{CD}}{\langle S\rangle_t} = \frac{4}{3\epsilon_{\mathrm{vac}}c^2}\frac{\omega_0\gamma_{21}\mathrm{Im}[\mathbf{m}_{21}\cdot(\hat{\mathcal{P}}^\dagger\boldsymbol{\mu}_{12})]}{|(\omega-\omega_0) + i\gamma_{21} - G|^2}, \tag{C3}$$

where ϵ_{vac} here is the vacuum permittivity, $\epsilon_r = \epsilon_0/\epsilon_{\mathrm{vac}}$, and c is speed of light in vacuum. Accordingly the CD signal in units of $\mathrm{M}^{-1}\mathrm{cm}^{-1}$ is given by

$$\Delta\varepsilon_{\mathrm{mol}} = \frac{N_A}{0.23}\Delta\sigma_{\mathrm{mol}} \tag{C4}$$

in which N_A is the Avogadro constant.

2. CD signal of NP part

The absorption rate of NPs is given by

$$Q_{\mathrm{NP}}(\omega) = \sum_i Q_i(\omega) = 2\omega\sum_i(\mathrm{Im}\epsilon_{\mathrm{NP}})\int|\mathbf{E}_{i\,\mathrm{tot}}|^2 dV, \tag{C5}$$

where ϵ_{NP} is the dielectric function of NPs; $\mathbf{E}_{i\,\mathrm{tot}}$ is the total electric field inside the ith sphere: $\mathbf{E}_{i\mathrm{tot}} = \mathbf{E}' - \frac{1}{4\pi\epsilon}\nabla\phi_{\mathrm{dipole}} = \mathbf{E}' - \frac{1}{4\pi\epsilon}\nabla(\mathbf{\Phi}^{\mathrm{tot}}\cdot\boldsymbol{\mu}_{12})\sigma_{21}$ in which ϵ_0 is the electric permittivity of space; and $\mathbf{\Phi}^{i,\mathrm{tot}}(\mathbf{r}) = \mathbf{\Phi}_0 + \mathbf{\Phi}_1 + \mathbf{\Phi}_2$ is the total electric potential in the ith sphere: $\mathbf{r} \in i$th sphere. Considering that $\mathrm{CD}_{\mathrm{NP}} = \langle Q_{\mathrm{NP},+} - Q_{\mathrm{NP},-}\rangle_\Omega$, thus we have

$$\mathrm{CD}_{\mathrm{NP}} = \mathrm{CD}_{\mathrm{NP,\,dipole\text{-}field}} + \mathrm{CD}_{\mathrm{NP,\,dipole\text{-}dipole}}, \tag{C6}$$

$$\mathrm{CD}_{\mathrm{NP,\,dipole\text{-}field}} = -\frac{\omega}{\pi\epsilon_0}\sum_i(\mathrm{Im}\epsilon_{\mathrm{NP}}) \times \mathrm{Re}\left\langle\int\left[(\mathbf{E}_i'^*\cdot\nabla\phi_{\mathrm{dipole},i})_+ - (\mathbf{E}_i'^*\cdot\nabla\phi_{\mathrm{dipole},i})_-\right]dV\right\rangle_\Omega, \tag{C7}$$

$$\mathrm{CD}_{\mathrm{NP,\,dipole\text{-}dipole}} = \frac{\omega}{8\pi^2\epsilon_0^2}\sum_i(\mathrm{Im}\epsilon_{\mathrm{NP}}) \times\left\langle\int[|\nabla\phi_{\mathrm{dipole},i}|^2{}_+ - |\nabla\phi_{\mathrm{dipole},i}|^2{}_-]dV\right\rangle_\Omega, \tag{C8}$$

where ± stands for the different incident directions $\mathbf{e}_{0\pm} = (\mathbf{e}_\theta \pm i\mathbf{e}_\phi)/\sqrt{2}$, ϵ_0 is the permittivity of space, and we have used $|\mathbf{E}_i'|_+^2 - |\mathbf{E}_i'|_-^2 = 0$.

Through simple algebra, one has

$$\langle\mathbf{E}'^*(\mathbf{r})\cdot\nabla\phi_{\mathrm{dipole}}(\mathbf{r})\rangle_{\Omega+} - \langle\mathbf{E}'^*(\mathbf{r})\cdot\nabla\phi_{\mathrm{dipole}}(\mathbf{r})\rangle_{\Omega-} = \frac{2\sqrt{\epsilon_r}}{3c}i|E_0|^2\frac{\mathbf{m}_{21}\cdot[\hat{K}^\dagger(\mathbf{r})\nabla(\mathbf{\Phi}^{\mathrm{tot}}(\mathbf{r})\cdot\boldsymbol{\mu}_{21})]}{\hbar(\omega-\omega_0) + i\gamma_{21} - G}, \tag{C9}$$

where we have used the enhancement factor $\hat{K}(\mathbf{r})$ [Eq. (B2)]: $\mathbf{E}'(\mathbf{r}) = \hat{K}(\mathbf{r})\mathbf{E}_0 = \mathbf{e}_0\hat{K}(\mathbf{r})E_0$ with $\mathbf{E}'(\mathbf{r})$ being the field induced only by the NP dimer in the position $\mathbf{r}$ inside spheres.

Substituting (C9) into (C7), we have

$$\mathrm{CD}_{\text{NP, dipole-field}} = \frac{2\omega\sqrt{\epsilon_r}}{3c\pi\epsilon_0}|E_0|^2\sum_i(\mathrm{Im}\epsilon_{\mathrm{NP}}) \times \mathrm{Im}\int\frac{\mathbf{m}_{21}\cdot[\hat{K}^{\dagger}(\mathbf{r})\nabla(\mathbf{\Phi}^{\mathrm{tot}}(\mathbf{r})\cdot\boldsymbol{\mu}_{21})]}{\hbar(\omega-\omega_0)+i\gamma_{21}-G}dV. \tag{C10}$$

Next, we calculate the second term of CD_{NP}: $\mathrm{CD}_{\text{dipole-dipole}}$. From Eqs. (A7) and (A8) we can see $\rho_{22}\propto|\sigma_{21}|^2$, so that $\mathrm{CD}_{\mathrm{mol}\pm}\propto\langle|\sigma_{21}|^2\rangle_{\Omega+}-\langle|\sigma_{21}|^2\rangle_{\Omega-}$. From Eq. (C2), we have

$$\langle|\sigma_{21}|^2\rangle_{\Omega+}-\langle|\sigma_{21}|^2\rangle_{\Omega-} = \frac{4\sqrt{\epsilon_r}}{3c}\frac{|E_0|^2\mathrm{Im}[\mathbf{m}_{21}\cdot(\hat{\mathcal{P}}^{\dagger}\boldsymbol{\mu}_{12})]}{|\hbar(\omega-\omega_0)+i\gamma_{21}-G|^2}, \tag{C11}$$

thus:

$$\begin{aligned}\mathrm{CD}_{\text{NP, dipole-dipole}} &= \frac{\omega}{8\pi^2\epsilon_0^2}\sum_i(\mathrm{Im}\epsilon_{\mathrm{NP}})(\langle|\sigma_{21}|^2\rangle_{\Omega+}-\langle|\sigma_{21}|^2\rangle_{\Omega-}) \times\int|\nabla(\mathbf{\Phi}^{\mathrm{tot}}\cdot\boldsymbol{\mu}_{21})|^2dV\\ &= \frac{\omega\sqrt{\epsilon_r}}{6\pi^2\epsilon_0^2c}\frac{|E_0|^2\mathrm{Im}[\mathbf{m}_{21}\cdot(\hat{\mathcal{P}}^{\dagger}\boldsymbol{\mu}_{12})]}{|\hbar(\omega-\omega_0)+i\gamma_{21}-G|^2}J(\omega),\end{aligned} \tag{C12}$$

where we have defined $J(\omega) = \sum_i(\mathrm{Im}\epsilon_{\mathrm{NP}})\int|\nabla(\mathbf{\Phi}^{\mathrm{tot}}\cdot\boldsymbol{\mu}_{21})|^2dV$, where $-\frac{1}{4\pi\epsilon_0}\nabla(\mathbf{\Phi}^{\mathrm{tot}}\cdot\boldsymbol{\mu}_{21})$ can be seen as the field induced by an effective molecular dipole $\boldsymbol{\mu}_{12}$. Thus, $J(\omega)$ has the meaning of energy rate. Specifically, in the presence of a molecule, the absorption rate of metal antiparticles due to energy transfer from molecule to spheres is given by $Q = \frac{2\omega}{16\pi^2\epsilon_0^2}\sum_i(\mathrm{Im}\epsilon_{\mathrm{NP}})\int|\nabla(\mathbf{\Phi}^{\mathrm{tot}}(\mathbf{r})\cdot\boldsymbol{\mu}_{12})|^2dV$; meanwhile the rate of energy transfer of molecule is given by $E = \omega\times 2\mathrm{Im}(-G) = -2\omega\mathrm{Im}G$. If we neglect the radiation from the system, then the energy conservation is satisfied, $Q = E$, with the result that $J(\omega) = -16\pi^2\epsilon_0^2\mathrm{Im}G$. Therefore, Eq. (C12) reduces to

$$\mathrm{CD}_{\text{dipole-dipole}} = -\frac{8\omega\sqrt{\epsilon_r}}{3c}\frac{|E_0|^2\mathrm{Im}[\mathbf{m}_{21}\cdot(\hat{\mathcal{P}}^{\dagger}\boldsymbol{\mu}_{12})]}{|\hbar(\omega-\omega_0)+i\gamma_{21}-G|^2}\mathrm{Im}G. \tag{C13}$$

Once $\mathrm{CD}_{\mathrm{NP}}$ is obtained [(C10) and (C13)], the CD signal in the standard units of $\mathrm{M}^{-1}\mathrm{cm}^{-1}$ can be obtained similarly to the derivation of $\mathrm{CD}_{\mathrm{mol}}$:

$$\begin{aligned}\Delta\sigma_{\mathrm{NP}} &= \frac{\mathrm{CD}_{\text{dipole-field}}+\mathrm{CD}_{\text{dipole-dipole}}}{\langle S\rangle_t},\\ \Delta\varepsilon_{\mathrm{NP}} &= \frac{N_A}{0.23}\Delta\sigma_{\mathrm{NP}}.\end{aligned} \tag{C14}$$

APPENDIX D: COMPARISON OF COMPONENTS OF CD SIGNAL

Next, we see the comparison of components of the CD signal. In Fig. 6 we show the three components of the CD signal at $\lambda_0 = 300$ nm and small distance $d = 1$ nm for gold NPs [Fig. 6(a)] and Ag NPs [Fig. 6(b)]. In such an off-resonant hybrid system, the chiral molecule usually does not absorb at the plasmonic wavelength, but it provides a chiral nonabsorbing environment for NPs because it is still optically active, with the result that the current inside NPs is chiral, and accordingly the CD signal occurs. Considering that the NPs are not chiral, thus $\mathrm{CD}_{\text{dipole-field}}$ and $\mathrm{CD}_{\text{dipole-dipole}}$ are totally due to the exciton-plasmon interaction between molecule and NPs. We can see clearly that a large plasmonic peak in the CD

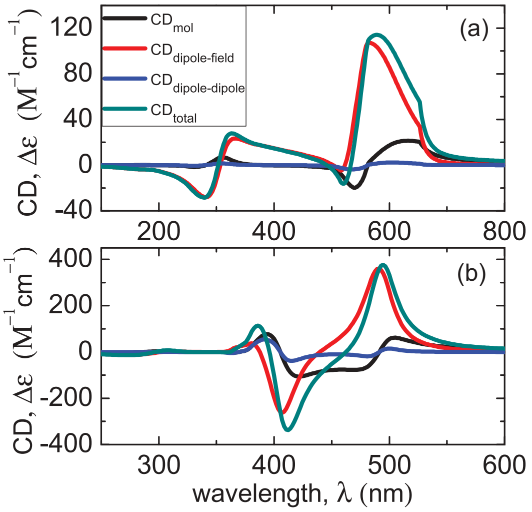

FIG. 6. (Color online) (a) The three components of the CD signal with varying λ under $\lambda_0 = 300$ nm and $d = 1$ nm for an Au dimer; (b) the same evolution of the CD signal for an Ag dimer. The molecule is placed in the center of the dimer, i.e., $\Delta = R + d/2$, and the other parameters are $R = 10$ nm, $\boldsymbol{\mu}||z$, $\lambda_0 = 300$ nm.

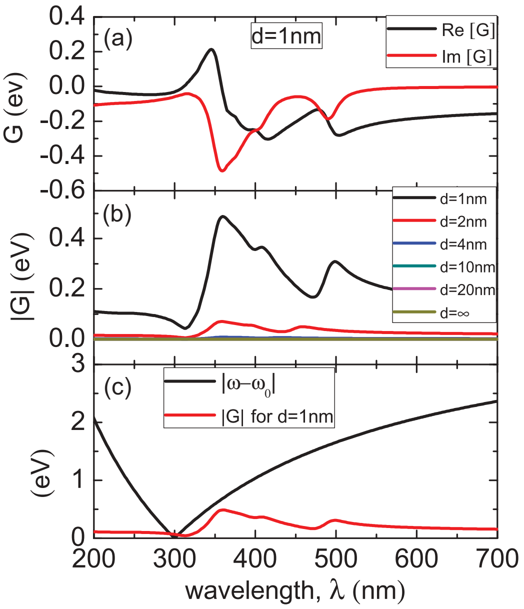

FIG. 7. (Color online) (a) The real and imaginary parts of the G function for $d = 1$ nm for a molecule–Ag-dimer system in the case $\boldsymbol{\mu}\perp z$; (b) the evolution of $|G|$ for diffirent d for the same system. (c) Comparison of $|\omega-\omega_0|$ and $|G|$ under $d = 1$ nm. Other parameters are the same as in Fig. 6.

spectrum emerges, while the $\mathrm{CD}_{\text{dipole-field}}$ term makes the main contribution. In fact, in the presence of a single NP rather than a dimer, CD_{mol} and CD_{NP} can be obtained analytically as[12,23] $\mathrm{CD}_{\text{mol}} \propto 1/\Delta\omega^2$, $\mathrm{CD}_{\text{NP}} \propto 1/\Delta\omega$ under large $\Delta\omega = \omega_0 - \omega$ and $|\Delta\omega| \gg \gamma_{12}$. In addition, $\mathrm{CD}_{\text{dipole-dipole}} \propto \mathrm{Im}G$ is usually very small in most cases unless d is very small, since $G \sim d^{-3}$. That is why $\mathrm{CD}_{\text{dipole-field}}$ determines the CD signal at the plasmon frequency in this case. To see it clearly, in Fig. 7 we show the order of the G function with varying separation d, from which we can see G is usually very small in most cases ($|G| \ll \gamma_{21},\omega_0$), and for not-small separation, $d \geqslant 2$ nm for example, it can even be ignored. At very small separation, such as $d = 1$ nm in our simulation where the giant CD effect can be observed, although here G is comparable with γ_{21} ($\mathrm{Re}G \ll \omega_0$, $\mathrm{Im}G \sim \gamma_{21}$), the influence of the G function is also small at the plasmon frequency and $\mathrm{CD}_{\text{dipole-field}}$ still dominates the main CD feature (see Fig. 6).

---

*zhangh@ohio.edu

†govorov@helios.phy.ohiou.edu

[1] M. Moskovits, Rev. Mod. Phys. **57**, 783 (1985).

[2] S. Nie and S. R. Emory, Science **275**, 1102 (1997).

[3] J. R. Lakowicz, Anal. Biochem. **298**, 1 (2001).

[4] *Circular Dichroism and the Conformational Analysis of Biomolecules*, edited by G. D. Fasman (Plenum, New York, 1996).

[5] M. Kuwata-Gonokami, N. Saito, Y. Ino, M. Kauranen, K. Jefimovs, T. Vallius, J. Turunen, and Y. Svirko, Phys. Rev. Lett. **95**, 227401 (2005).

[6] I. Lieberman, G. Shemer, T. Fried, E. M. Kosower, and G. Markovich, Angew. Chem. Int. Ed. Engl. **47**, 4855 (2008).

[7] J. George and K. G. Thomas, J. Am. Chem. Soc. **132**, 2502 (2010).

[8] Z. Li, Z. Zhu, W. Liu, Y. Zhou, B. Han, Y. Gao, and Z. Tang, J. Am. Chem. Soc. **134**, 3322 (2012).

[9] E. Hendry, T. Carpy, J. Johnston, M. Popland, R. V. Mikhaylovskiy, A. J. Lapthorn, S. M. Kelly, L. D. Barron, N. Gadegaard, and M. Kadodwala, Nat. Nanotechnol. **5**, 783 (2010).

[10] S. Zhang, H. Wei, K. Bao, U. Hakanson, N. J. Halas, P. Nordlander, and H. Xu, Phys. Rev. Lett. **107**, 096801 (2011).

[11] V. A. Gérard, Y. K. Gun'ko, E. Defrancq, and A. O. Govorov, Chem. Commun. **47**, 7383 (2011).

[12] A. O. Govorov, Z. Fan, P. Hernandez, J. M. Slocik, and R. R. Naik, Nano Lett. **10**, 1374 (2010).

[13] Z. Fan and A. O. Govorov, Nano Lett. **10**, 2580 (2010).

[14] J. M. Slocik, A. O. Govorov, and R. R. Naik, Nano Lett. **11**, 701 (2011); B. M. Maoz, R. van der Weegen, Z. Fan, A. O. Govorov, G. Ellestad, N. Berova, E. W. Meijer, and G. Markovich, J. Am. Chem. Soc. **13**, 17807 (2012).

[15] R.-Y. Wang, H. Wang, X. Wu, Y. Ji, P. Wang, Y. Qu, and T.-S. Chung, Soft Matter **7**, 8370 (2011).

[16] N. Cathcart and V. Kitaev, ACS Nano **5**, 7411 (2011).

[17] V. V. Klimov, D. V. Guzatov, and M. Ducloy, Europhys. Lett. **97**, 47004 (2012).

[18] M. Hentschel, M. Schäferling, T. Weiss, N. Liu, and H. Giessen, Nano Lett. **12**, 2542 (2012); M. Hentschel, M. Schäferling, B. Metzger, and H. Giessen, *ibid.* (2012), doi:10.1021/nl3041355.

[19] A. Kuzyk, R. Schreiber, Z. Fan, G. Pardatscher, E.-M. Roller, A. Högele, F. C. Simmel, A. O. Govorov, and T. Liedl, Nature (London) **483**, 311 (2012).

[20] Z. Zhu, W. Liu, Z. Li, B. Han, Y. Zhou, Y. Gao, and Z. Tang, ACS Nano **6**, 2326 (2012).

[21] Z. Xu, L. Xu, Y. Zhu, W. Ma, H. Kuang, L. Wang, and C. Xu, Chem. Commun. **48**, 5760 (2012).

[22] W. Yan, L. Xu, C. Xu, W. Ma, H. Kuang, L. Wang, and N. A. Kotov, J. Am. Chem. Soc. **134**, 15114 (2012).

[23] A. O. Govorov, J. Phys. Chem. C **115**, 7914 (2011).

[24] L. D. Barron, *Molecular Light Scattering and Optical Activity*, 2nd ed. (Cambridge University Press, Cambridge, UK, 2004).

[25] See Supplemental Material at http://link.aps.org/supplemental/10.1103/PhysRevB.87.075410 for a description of the quadrupole contribution to the total CD signal and for additional data on the absorption rate of Ag dimer.

[26] A. O. Govorov, G. W. Bryant, W. Zhang, T. Skeini, J. Lee, N. A. Kotov, J. M. Slocik, and R. R. Naik, Nano Lett. **6**, 984 (2006).

[27] E. D. Palik, *Handbook of Optical Constants of Solids* (Academic, New York, 1985).

[28] E. Hao and G. C. Schatz, J. Chem. Phys. **120**, 357 (2004).

[29] F. J. G. de Abajo, J. Phys. Chem. C **112**, 17983 (2008).

[30] S. Savasta, R. Saija, A. Ridolfo, O. D. Stefano, P. Denti, and F. Borghese, ACS Nano **4**, 6369 (2010).

[31] W. Zhang, A. O. Govorov, and G. W. Bryant, Phys. Rev. Lett. **97**, 146804 (2006).

[32] D. Neuhauser and K. Lopata, J. Chem. Phys. **127**, 154715 (2007).

[33] L. D. Barron, Mol. Phys. **21**, 241 (1971).

[34] N. A. Abdulrahman, Z. Fan, T. Tonooka, S. M. Kelly, N. Gadegaard, E. Hendry, A. O. Govorov, and M. Kadodwala, Nano Lett. **12**, 977 (2012).

[35] J. Zuloaga, E. Prodan, and P. Nordlander, Nano Lett. **9**, 887 (2009); R. Esteban, A. G. Borisov, P. Nordlander, and J. Aizpurua, Nat. Commun. **3**, 825 (2012).